# Preparation of solution-grown lozenge-shaped poly(*p*-phenylene terephthalamide) single crystals and their structural stabilization by heat treatment

Tetsuya Uchida*, Yutaro Hara, Tomoyasu Takaki

* Corresponding author. Graduate School of Natural Science and Technology,

Okayama University, 3-1-1 Tsushima-naka, Kita-ku Okayama 700-8530, Japan

E-mail address: tuchida@cc.okayama-u.ac.jp (T.Uchida)

*Keywords:* Poly(*p*-phenylene terephthalamide); Single crystals; Heat treatment

Highlights

- Lozenge-shaped poly(*p*-phenylene terephthalamide) single crystals were obtained.
- The PPTA single crystals consisted of modification I crystals.
- The single crystal thickness was approximately equal to the PPTA chain length.
- Upon the single crystal heat treatment, the symmetry changed from P1a1 to P11n.
- The heat treatment did not change the thickness of the PPTA single crystals.

# ABSTRACT

In this study, the preparation of poly (*p*-phenylene terephthalamide) (PPTA) single crystals was examined using crystallization from dilute solutions in concentrated sulfuric acid. Lozenge-shaped PPTA single crystals were successfully prepared using a self-seeding method with a low degree of supercooling, and they consisted of modification I crystals. The *a*-axis direction of the crystal corresponded to the long diagonal direction of the rhombus, the *b*-axis direction with the short diagonal direction, and the PPTA molecular chain direction (the *c*-axis direction) with the crystal's thickness direction. In addition, the PPTA single crystals had a (110) growth plane, where the thickness of each single crystal was approximately equal to the molecular chain length of the PPTA. Upon heat treatment of the PPTA single crystals, the symmetry changed from P1a1 to the more stable P11n. In addition, the heat treatment caused a difference in the density of each symmetric crystal, resulting in crack formation along the *b*-axis direction, which is the hydrogen-bonding direction. However, the heat treatment did not change the thickness of the PPTA single crystals. Conversely, the isothermal crystallization of the PPTA caused progression in the crystallization only under a high degree of supercooling, thus yielding plate-like PPTA crystals that consisted of modification II crystals. In these plate-like PPTA crystals, the length corresponded to the crystal *a*-axis direction, and the electron diffraction pattern was broad. Furthermore, the equilibrium dissolution temperature of the PPTA single crystals was discussed.

# 1. Introduction

Poly(*p*-phenylene terephthalamide) (PPTA) is a rigid polymer whose molecular chains cannot fold, and it is widely used as high-performance fibers and films possessing high tensile strength, high elastic modulus, high thermal resistance, and good chemical resistance [1–10]. Various studies have attempted to elucidate the crystal structure and crystallization mechanisms of PPTA. Northolt *et al*. [11, 12] revealed the crystallographic structure of PPTA fibers using X-ray structural analysis. Subsequently, Haraguchi *et al*. [13] reported the crystalline structure of PPTA films prepared from sulfuric acid solutions, which was different from that proposed by Northolt *et al*. These proposed structures were called modification I and modification II, respectively. In a study by Dobb *et al*. [14], the molecular chain orientation and microstructure of PPTA crystals were clarified by observing PPTA fibers. The *b*-axis direction corresponding to the hydrogen-bonding direction was oriented in the radial direction throughout the solidification process during spinning, and the sheet structures grown in the *b*- and *c*-axis directions existed in the fibers. They concluded that the sheet structure was formed via hydrogen bonding and it was the basic structure for the PPTA fiber, named the pleated sheet model. However, PPTA fiber structure is quite complicated and these results obtained from fibers are not enough to clarify the characteristics of PPTA crystallization by studying only the fiber.

In order to clarify the crystallization behavior of PPTA, it is important to understand the morphology and growth mechanism of PPTA single crystals. Additionally, the structural stabilization of PPTA single crystals through heat treatment is valuable not only from an academic but also an industrial perspective. Various techniques for the preparation of PPTA single crystals have been previously reported. Liu *et al*. [15] prepared a PPTA single crystal using the confined thin film melt polymerization method, resulting in the formation of lath-

shaped modification I crystals with the long axis of the laths corresponding to the *b*-axis, which is the hydrogen-bonded direction. Takahashi *et al*. [16] prepared negative PPTA spherulites using strain-induced crystallization from a sulfuric acid solution, and the prepared crystals consisted of “fibrous” lamellae of several tens of nanometers. The molecular chain axes were perpendicular to the long axis of each lamella, and the long axis of the “fibrous” lamellae corresponded to the *b*-axis. Jackson *et al*. [17] performed high-temperature PPTA crystallization in organic solutions induced by the addition of a poor solvent or precipitating agent, and they reported that PPTAs with a molecular weight (Mw) of 46,000 afforded ribbon-like crystals and those with a Mw of 3,430 afforded small needle-like crystals. Both crystals were the modification I structures. With higher molecular-weight PPTA, the molecular chain axes were parallel to the ribbon axes in an extended-chain-type structure. These results revealed that PPTA could form extended chain crystals with lamellar or ribbon-like morphologies. In the lamellar crystals, the molecular chains were oriented perpendicular to the plate surface, and the length direction of the crystals corresponded to the *b*-axis direction, which was the hydrogen-bonding direction. This result indicated that the formation of hydrogen bonds affected the crystal growth. However, the PPTA crystal growth plane was not clarified in previous studies.

In this study, single crystals were crystallized from dilute PPTA solutions, and the relationship among the morphology, growth direction, crystal system, and microstructure of the obtained PPTA single crystals was investigated. Subsequently, the PPTA single crystals were subjected to heat treatment to examine the properties associated with structural stabilization. Furthermore, the equilibrium dissolution temperature of the PPTA single crystals was examined.

# 2. Experimental Section

## 2.1. PPTA Samples

PPTA samples of different Mw were prepared by the hydrolysis of PPTA fibers (Kevlar, DuPont de Nemours, Inc., DE, USA) [18]. The fibers were washed with methanol and dried *in vacuo*. Then, they were placed in a 10 M aqueous solution of sodium hydroxide, and the mixture was refluxed at 135°C for a predetermined period. The resulting residues were washed with distilled water and dried *in vacuo* at 135°C. The Mw of the PPTA samples was calculated from their intrinsic viscosities, which were measured in 96.6 wt% sulfuric acid at 25°C using the following equation [19]:

$$[\eta] = 1.95 \times 10^{-6} M_W{}^{1.36}.$$

The molecular length (L) of each PPTA sample was calculated from its Mw, where the repeating unit length ($L_0$) was 1.29 nm [11]. Also, the Mw was controlled by the hydrolysis time. The results are presented in Table 1. The Mw and molecular lengths of the PPTAs in Table 1 represent the average Mw and molecular chain length obtained from the conducted viscosity measurements. Thus, the used PPTA samples in this study are polydisperse. Four PPTA samples were prepared with different L's of 32, 60, 80, and 220 nm, which were calculated from the Mw, and the samples were called PPTA(32), PPTA(60), PPTA(80), and PPTA(220), respectively.

**Table 1** Relationship between the hydrolysis time and the molecular length.

| Hydrolysis time (h) | [η] | $M_w$ | $DP_n$[a] | Molecular length (L) (nm)[b] | Sample code |
|---|---|---|---|---|---|
| 0 | 3.62 | 40,600 | 171 | 220 | PPTA(220) |
| 24 | 0.92 | 14,800 | 62 | 80 | PPTA(80) |
| 35 | 0.60 | 10,900 | 46 | 60 | PPTA(60) |
| 78 | 0.26 | 5900 | 25 | 32 | PPTA(32) |

[a] Average degree of polymerization.

[b] Monomer length estimated with $L_o$ of 1.29 nm [11].

## 2.2. Preparation of PPTA Single Crystals

The PPTAs were dissolved in 78.5 wt% sulfuric acid in a concentration of 0.1 wt% at 120°C. Then, the solution was kept at a predetermined temperature to obtain the PPTA crystals through conventional isothermal crystallization. Furthermore, crystallization using the self-seeding method [21] was carried out in the following procedure. First, the PPTA crystal suspensions, which were prepared using isothermal crystallization at 30°C, were heated from 30°C at a rate of 12°C/h until the turbidity disappeared, resulting in the apparent dissolution of crystals. Thereafter, the solution was immediately cooled to the crystallization temperature, and the precipitates were then washed with distilled water until a neutral pH was obtained.

## 2.3. Measurements

Isothermal crystallization was conducted at the predetermined temperature, whereas the time-to-cloudiness of the solution was measured using visual confirmation as the time at

which the solution became cloudy, indicating the crystals growth to submicron sizes. Also, each PPTA crystal suspension was heated at a rate of 6°C/h, and the dissolution temperature ($T_d$) of the PPTA crystals was visually observed, at which the solution transitioned from the cloudy state to a clear one. The measurements were performed three or more times under each set of conditions. Under the analogous conditions, the same time-to-cloudiness and the $T_d$ were noted within the effective digit.

## 2.4. Transmission Electron Microscopy and Scanning Probe Microscopy Observation

The samples were prepared for a transmission electron microscope (TEM) and scanning probe microscopy imaging by depositing the precipitate suspensions in water onto carbon grids or mica plates and then by drying in air at room temperature. The morphologies and electron diffraction patterns of the PPTA crystals were observed by the TEM (JEM2000EXII manufactured by JEOL Ltd. Tokyo, Japan) at an acceleration voltage of 200 kV, and their morphologies and thickness were observed in ScanAsyst modes using a scanning probe microscope (SPM; Multi Mode 8, manufactured by Bruker Co., MA, USA).

## 2.5. Heat Treatment of PPTA Crystals

The PPTA crystal suspension was dropped onto a TEM observation grid made of a supporting silicon nitride membrane substrate (S171-1; Agar Scientific Ltd., Essex, UK) or onto an SPM observation substrate (mica), and it was then dried at 25$^{o}$C. Thereafter, using a vacuum heating furnace (FT-101S; Full-tech Co., Osaka, Japan), heat treatment was performed at a predetermined temperature *in vacuo*.

# 3. Results and Discussion

## 3.1. Preparation and Structure of PPTA Single Crystals

The PPTA(220) did not dissolve in 78.5 wt% sulfuric acid at a concentration of 0.1 wt% at 25°C; however, it dissolved after it was heated to 140°C. Even when the PPTA(220) solution was cooled to 0°C, crystallization was not observed. However, the PPTA(32), PPTA(60), and PPTA(80), which were composed of shorter molecular chains, effectively dissolved in 78.5 wt% sulfuric acid at a concentration of 0.1 wt% at 120°C. Subsequently, when the solution was cooled to 0°C, cloudiness in the solution was noted in all the samples after 1 h, which indicates crystallization. To gain a better understanding of these results, we referred to the outcomes of some previous investigations that considered other rigid polymers.

It was reported that rigid polymers, such as poly(*p*-phenylene benzobisthiazole) (PBZT) and poly(*p*-phenylene benzobisoxazole) (PBO), can be crystallized from dilute solutions by isothermal crystallization [22–25]. Both PBZT and PBO are rigid polymers composed of a heterocycle and a benzene ring. These molecules do not contain any amide bonds; therefore, in contrast to PPTA molecules, they exhibit lower flexibility and are less affected by intermolecular hydrogen bonding than PPTA molecules. Moreover, in a previous study considering PBZT [23], instantaneous crystallization was observed when the polymer was dissolved at a concentration of 0.1 wt% at 120°C and then quenched to 0°C. However, in the case of PPTA, such instantaneous crystallization was not observed under any crystallization conditions. These results indicate that the crystal growth rate of PPTA is significantly slower than that of PBZT. This difference can be attributed to the lower rigidity of the molecular chains of PPTA in comparison with the molecular chains of PBZT, which is due to the presence of an amide bond in PPTA molecules. In addition, studies involving PBZT revealed that the crystal growth rate is usually slow for long and rigid molecular chains with the same

degree of supercooling ($D_{sp}$), which is defined as the difference between the $T_d$ and the crystallization temperature. Hence, it was concluded that crystallization hardly takes place in long-chain PPTA molecules, such as the PPTA(220). Consequently, the PPTA(32), PPTA(60), and PPTA(80) were used in the subsequent study, as they exhibit relatively shorter molecular chains.

The $T_d$s of the PPTA(32), PPTA(60), and PPTA(80), which were obtained by quenching to 0°C, are 95.8°C, 101.0°C, and 103.2°C, respectively. It can be seen that longer PPTA molecular chains have higher $T_d$s. The $T_d$ of PPTA crystals will be discussed later in the manuscript. The relationship between the isothermal crystallization temperatures and the times-to-cloudiness of the PPTA samples is demonstrated in Table 2. With the same crystallization temperature, crystallization occurred more rapidly in the solution with the longer molecular chains. Thus, it can be concluded that $D_{sp}$ determines the crystallization behavior. Therefore, for the same molecular chain length, a longer time is needed for crystallization at higher temperatures. In addition, it was clarified that crystallization did not occur at $D_{sp} \leqq 33$°C using the abovementioned conventional isothermal crystallization.

**Table 2** Relationship between the crystallization temperature and the time-to-cloudiness.

| Crystallization temperature (°C) | Time-to-cloudiness (h) | | |
|---|---|---|---|
| | PPTA(32) | PPTA(60) | PPTA(80) |
| 0 | 1 | 1 | 1 |
| 30 | 3 | 2 | 1.5 |
| 40 | 5.5 | 5 | 4 |
| 60 | 40 | 13.5 | 12.5 |
| 65 | NC [a] | 18 | 15 |
| 70 | NC | 22.5 | 19 |
| 75 | NC | NC | NC |

[a] Crystallization did not occur.

Subsequently, isothermal crystallization was carried out using a self-seeding method [21]. When the PPTA(32) solution was kept at 65°C after using the conventional isothermal crystallization method, crystallization was not observed, as shown in Table 2. However, by using the self-seeding method, crystallization was observed in 20 min at 65°C ($D_{sp}$ = 30.8°C) in the PPTA(32) solution, as shown in Table 3. The observed time-to-cloudiness by the self-seeding method was extremely shorter than that observed by the conventional isothermal crystallization method. These results revealed that undissolved crystals serve as nuclei and that the self-seeding method works for the preparation of PPTA crystals with a low $D_{sp}$. Similarly, in the PPTA(60) and PPTA(80) solutions, crystallization was observed at 75°C after using the self-seeding method, but it was not observed at 75°C after using the conventional isothermal crystallization method.

From these results, it was found that crystal growth was mainly controlled by the primary nucleation in the crystallization from dilute solutions of PPTA. After the primary nuclei were formed, subsequent secondary nucleation and crystal growth were found to occur almost immediately. In addition, the molecular chain length of PPTA had a considerable effect on the crystallization temperature and crystal growth rate.

**Table 3** Relationship between the self-seeding crystallization temperature and the time-to-cloudiness.

| Crystallization temperature (°C) | Time-to-cloudiness (min) | | |
|---|---|---|---|
| | PPTA(32) | PPTA(60) | PPTA(80) |
| 65 | 20 | 6 | 3 |
| 75 | NC [a] | 20 | 18 |
| 80 | NC | NC | NC |

[a] Crystallization did not occur.

To clarify the morphology and crystal structure of the obtained crystals, TEM observation was conducted. The isothermal crystallization of PPTA(32) at 60°C ($D_{sp}$ = 35.8°C) yielded thin plate-like crystals, as shown in Figure 1a. The selected area electron diffraction pattern of this plate-like crystal exhibited diffuse arc-shape streaks, as shown in Figure 1b, which indicates that the crystal orientation in this plate-like crystal is disordered. The d-spacing values were calculated from the electron diffraction patterns (Supporting Information, Table S1), and these reflections could be indexed as modification II PPTA crystals, as reported by Xu *et al*. [26]. It was also found that the crystal's length direction corresponded to the crystalline *a*-axis, whereas the crystal's width direction corresponded to its *b*-axis, which is the hydrogen-bonding direction. Also, the molecular chains were oriented perpendicular to the plate. These results differ from those obtained in a previous study [15], wherein the PPTA crystals, prepared using the confined thin-film melt polymerization method, were grown in the *b*-axis direction, indicating the strong influence of hydrogen bonding between the PPTA molecular chains in the crystal growth direction.

On the other hand, the isothermal crystallization of PPTA(32) at 0°C ($D_{sp}$ = 95.8°C) resulted in the formation of fan-like aggregates of ribbon-like lamellae, as shown in Figure 1c. Similar morphology was observed in the isothermal crystallization of the PPTA(32) at 30°C ($D_{sp}$ = 65.8°C), as shown in Figure 1d. The electron diffraction pattern of the ribbon-like lamellar crystals was unclear, but it was similar to that of the plate-like crystals. Therefore, the crystal's length direction corresponded to the crystalline *a*-axis, whereas its width direction corresponded to the *b*-axis. The molecular chains were also oriented perpendicular to the plate.

These results indicate that metastable modification-II PPTA crystals were obtained from dilute solutions of PPTA in a sulfuric-acid solution having a large $D_{sp}$. The crystal's length increased in the *a*-axis direction. It is considered that during the crystallization in the sulfuric

acid solution, the effect of the hydrogen bonding between the PPTA molecular chains was weakened by the interaction between the PPTA molecular chains and sulfuric acid, and the growth in the *b*-axis direction did not proceed predominantly.

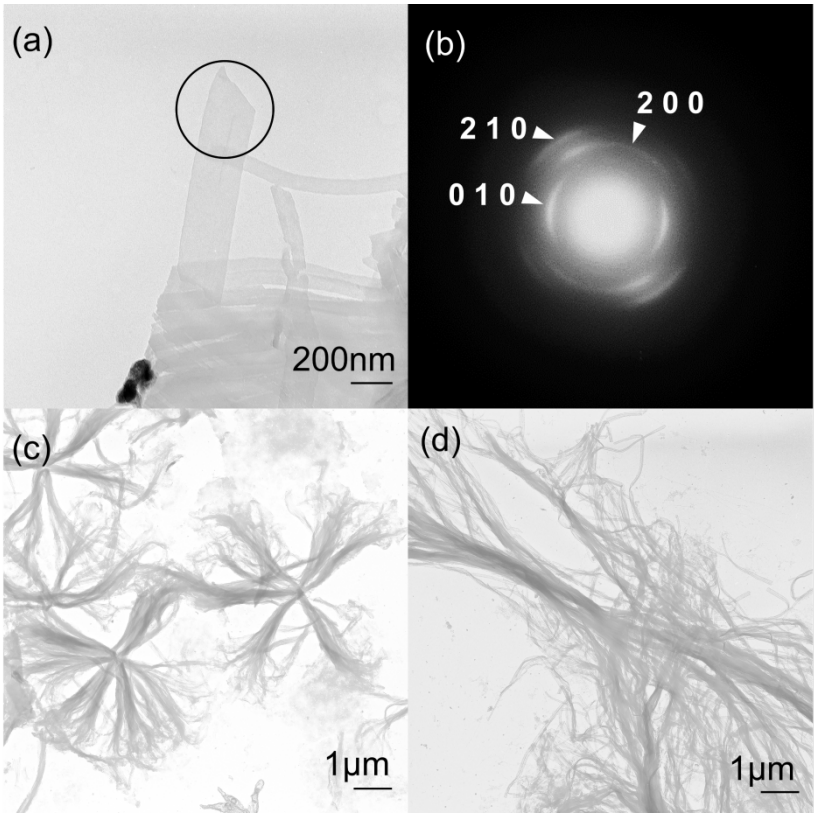


**Figure 1.** Transmission electron microscopy images of PPTA(32) crystals. a) isothermally crystallized at 60°C, b) electron diffraction image taken from the circled area in a), c) isothermally crystallized at 0°C, and d) isothermally crystallized at 30°C.

The bright-field image and electron diffraction pattern of the prepared PPTA(32) crystal using the self-seeding method at 65°C ($D_{sp}$ = 30.8°C) are shown in Figure 2a and b, respectively. As seen in the figure, a lozenge-shaped morphology and sharp spots in the electron diffraction pattern can be observed. All the spots were indexed with an orthorhombic unit cell of $a$ = 0.788 nm, $b$ = 0.522 nm, and $c$ = 1.29 nm, corresponding to the fiber axis (Supporting Information, Table S2). These results indicate the following: the product is a

modification I PPTA crystal, as reported by Northolt [12] and Liu [15], the molecular chains oriented perpendicular to the lamella, and the crystalline *a*-axis is along the long diagonal direction, whereas the crystalline *b*-axis is along the short diagonal direction. Furthermore, the crystal's (110) plane corresponds to the growth direction of the single crystal.

The morphology and electron diffraction pattern of the prepared PPTA(80) single crystal by the self-seeding method at 75°C ($D_{sp}$ = 28.2°C) are shown in Figures 2c and d, respectively. As seen in the figure, they are similar to those of the PPTA(32) single crystals. The PPTA(60) single crystals (Supporting Information, Figure S2) are also similar to the PPTA(32) and PPTA(80) single crystals. Thus, the metastable modification II crystals were obtained as lamellar crystals with relatively high degrees of supercooling ($D_{sp}$ > 33°C), whereas the stable PPTA modification I crystals were obtained as lozenge-shaped single crystals with relatively low degrees of supercooling ($D_{sp}$ < 31°C). The crystal habit of the lozenge-shaped PPTA single crystals was plainly evident, and the growth plane of the PPTA single crystal was the (110) plane. In this case, the crystal growth direction was defined by the crystal unit cell and was not affected by hydrogen bonding. Thus, crystallization using the self-seeding method under a relatively low degree of supercooling is required to prepare lozenge-shaped PPTA single crystals.

As described, the effect of the hydrogen bonding between the PPTA molecular chains was weakened through the crystallization in the sulfuric acid solution, and crystallization at a small $D_{sp}$ could be conducted using the self-seeding method. Thus, a lozenge-shaped PPTA single crystal was obtained wherein the (110) planes were reflected in the crystal's growth plane.

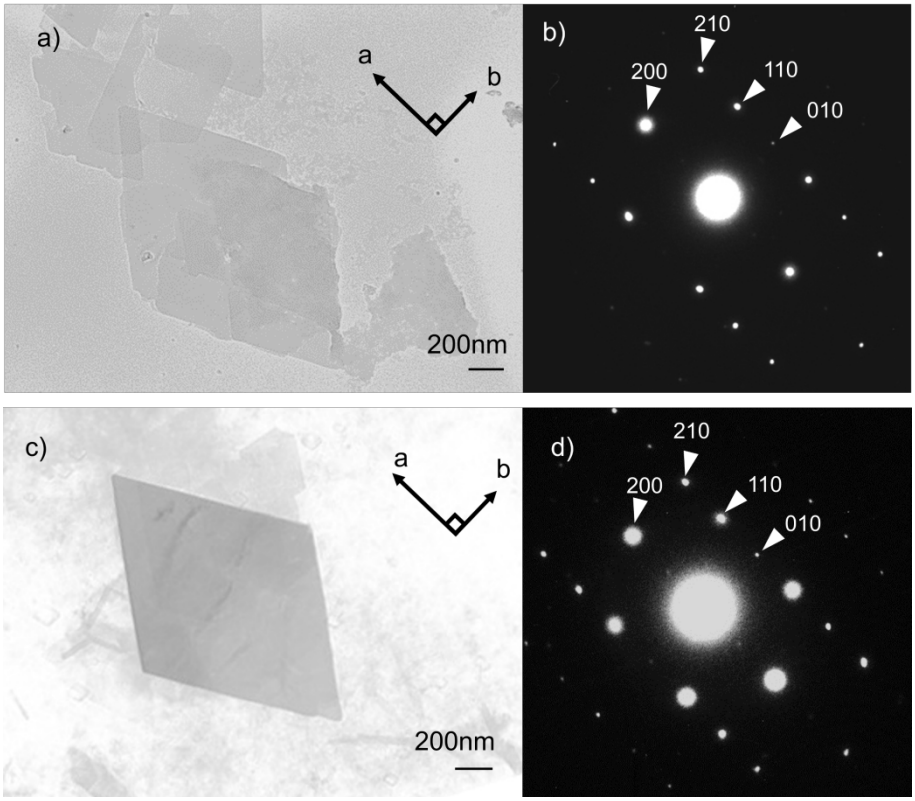


**Figure 2.** Transmission electron microscopy and electron diffraction of PPTA single crystals. a) PPTA(32) single crystal prepared using the self-seeding method at 65°C, b) electron diffraction from the selected area in a), c) PPTA(80) single crystal prepared using the self-seeding method at 75°C, and d) electron diffraction from the selected area in c)

Dark-field images taken by the 200 and 110 reflections of the PPTA(32) single crystals are presented in Figures 3a and b, respectively. A pattern of stripes parallel to the short diagonal direction (the *b*-axis) can be observed in the dark-field image of a lozenge-shape crystal taken by the 200 reflection. Conversely, in the dark-field image taken by the 110 reflection, crystallites can be observed all over the crystal. In the lozenge-shape single crystals prepared by crystallization from a dilute solution of polyethylene [27], a dark-field image, taken by the 110 reflection, exhibited bright diagonal sectors [28]. This pattern is

attributed to the fact that the polyethylene single crystal has a hollow pyramidal structure and that the molecular chains in each sector have different folding directions, resulting in a diagonal extinction in the 110 dark-field image. In contrast, in the 110 dark-field image of the PPTA single crystal, such diagonal extinctions do not exist, which indicates that the PPTA single crystal was formed of extended molecular chains; therefore, there were no folded structures on the crystal surface, and the crystal did not have a hollow pyramid structure like the polyethylene single crystal.

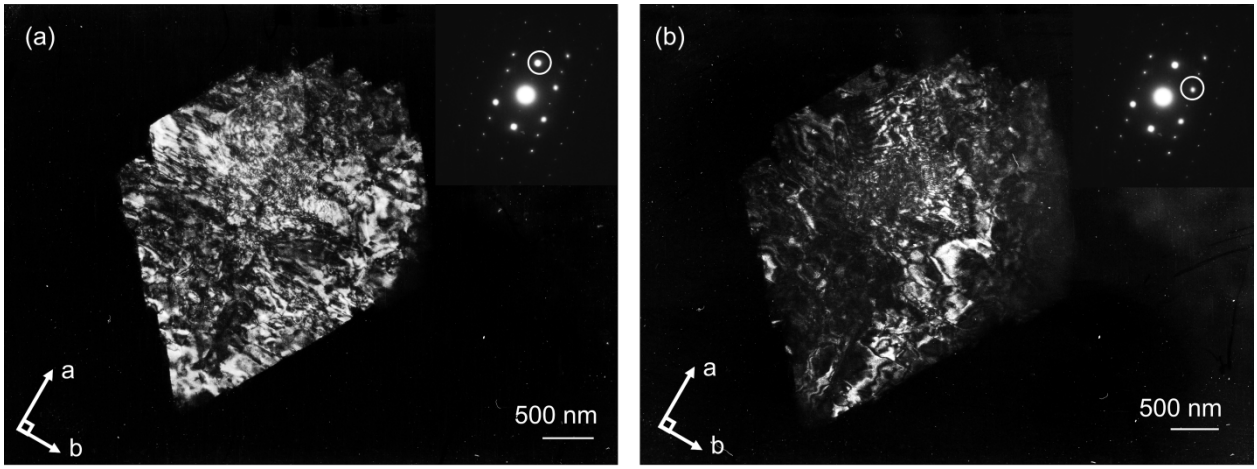


**Figure 3.** Dark-field images of the PPTA(32) single crystal taken by the a) 200 reflection and b) 110 reflection.

A scanning probe microscopy image of the PPTA(32) single crystal, which was prepared using the self-seeding method at 65°C, is shown in Figure 4a. As shown in Figure 2a, a lozenge-shaped crystal can be observed. Occasionally, the overgrowth of lamellar crystals is observed in some regions. Therefore, the thickness measurements of the PPTA single crystal were conducted at locations corresponding to the thickness of a single sheet of the lamellar crystal. The measured crystal thickness was about 40 nm, as shown in Figure 4b, which is close to the average molecular chain length (32 nm) of the used PPTA for crystallization. An image of the prepared PPTA(80) single crystal using the self-seeding method at 75°C is

shown in Figure 4c. The thickness of the crystal was about 80 nm (Figure 4d), which is the same as the average molecular chain length (80 nm) of the used PPTA for crystallization. These results clarified that the thickness of the PPTA single crystals that have a clear crystal habit is close to the average molecular chain length of the used PPTA for crystallization. In other words, it was found that there is no difference in the crystal habits of the obtained single crystals, even when the molecular chain length varied in the range of the molecular chain length of the used PPTAs in this study. Since each PPTA single crystal is composed of an extended chain, the difference in the molecular chain length is directly reflected only in the thickness of single crystals. Thus, the following discussion concerning the heat treatment of the PPTA single crystals is based on the obtained results for the PPTA(32) crystals; however, the results are also analogous to other PPTA crystals.

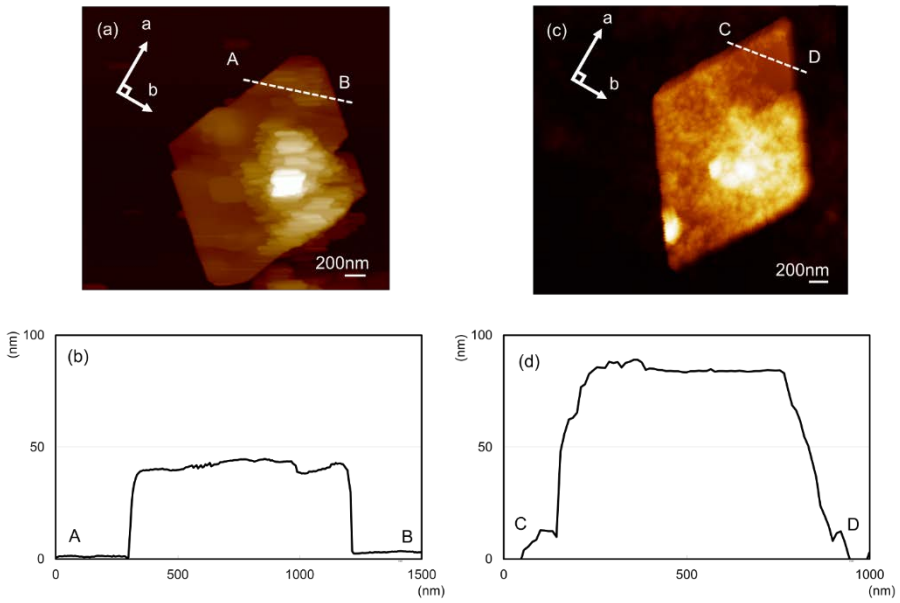


**Figure 4.** Scanning probe microscopy images and cross-sectional height profiles of PPTA single crystals. a) PPTA(32) single crystal prepared by the self-seeding method at 65°C, b) the cross-sectional height profile along the line A–B in a), c) PPTA(80) single crystal prepared by the self-seeding method at 75°C, and d) the cross-sectional height profile along the line C–D in c).

## 3.2. Heat Treatment of PPTA Single Crystals

The PPTA(32) single crystals were heat-treated at 350°C, and the change in the morphology is shown in Figure 5. Cracks were observed parallel to the *b*-axis, and these cracks were attributed to the formation of hydrogen-bonded sheets in the crystals. The electron diffraction images before and after the heat treatment are shown in Figure 6. The $h + k$ = odd (i.e., *hk0*) reflections disappeared, whereas the intensities of the 200 and 310 reflections were increased by the heat treatment. In addition, the results of the X-ray diffraction pattern of the as-crystallized and heat-treated PPTA single crystals were the same as those of the electron

diffraction pattern (Supporting Information, Figure S3.) From these results, it can be concluded that the symmetry of the PPTA crystals changed during the heat treatment. In addition, the modification I PPTA crystal structures were reported to have a P1a1 symmetry with respect to the *b*-axis direction [15] and a P11n symmetry with respect to the *c*-axis direction [11, 12, 15]. In the P11n symmetry, the adjacent molecular chains in the diagonal direction can be regarded as equivalent, so the *hk0* reflections can be considered to have canceled each other out. In contrast, in the P1a1 symmetry, the adjacent molecular chains in the diagonal direction cannot be regarded as equivalent, so the *hk0* reflections cannot completely cancel each other out. According to the electron diffraction images before and after the heat treatment, which coincide with the P1a1 and P11n symmetries, respectively, the symmetry of the crystal changed from P1a1 to P11n. The hydrogen-bonding (N–H–O) distances and angles of the P1a1 and P11n symmetry crystals were also determined [15]: the distances and angles of the hydrogen bonds of the P1a1 symmetry crystal are 0.2328 nm and 155.2°, respectively, while those of the hydrogen bonds of the P11n symmetry crystal are 0.2124 nm and 172°, respectively. Therefore, the distance of the hydrogen bond is closer in the P11n symmetry crystal than in the P1a1 symmetry crystal, and the angle of the hydrogen bond of the P11n symmetry crystal is more linear than that of the P1a1 symmetry crystal. Based on these results, it was concluded that the intermolecular hydrogen bonding in the crystal region gets stronger after heat treatment. In Ref. 15, the unit cells of the P11n symmetry crystal and the P1a1 symmetry crystal were reported as follows: P11n ($a$ = 0787 nm, $b$ = 0.518 nm, $c$ = 1.29 nm) and P1a1 ($a$ = 0.788 nm, $b$ = 0.522 nm, $c$ = 1.29 nm). Hence, the P11n symmetry crystal is denser than the P1a1 symmetry crystal. It was also considered that the crystal densification following the heat treatment made it difficult to maintain the original morphology and that the van der Waals forces in the *a*-axis direction were weaker than the hydrogen bonding in the *b*-axis direction, thus resulting in the formation of cracks

parallel to the *b*-axis. This change in the symmetry was attributed to a 1/2 shift in the molecular chain along the molecular chain axis [15]. Such cracks and changes in the crystal symmetry were observed when the heat treatment was performed at 300°C, 350°C, and 400°C. In Ref. 29, the β*-relaxation around 250°C was reported in a study on the dynamic mechanical properties of PPTA fibers, which was determined to be associated with the thermal molecular motion in the crystalline region. In addition, in a study on the dynamic mechanical properties of PPTA fibers, Kunugi *et al.* also reported that the β*-relaxation was observed at approximately 270°C [30]. Moreover, it was also reported that the crystallinity of Kevlar fibers increased after heat treatment at 300°C. Hindeleh *et al*. also reported that the crystallinity and the microparacrystallite (mPC) size of Kevlar fibers increased after heat treatment at a temperature of at least 250°C [31]. These results indicate that the heat treatment of >250°C results in a molecular motion of the molecular chains of crystal regions and leads to structural changes not only in the amorphous region but also in crystal regions. Although it is not directly established that molecular motion in the molecular chain axis direction is present, it is inferred that the molecular motion in the molecular chain axis direction is generated by heat treatment at 250°C or higher. This is based on the X-ray diffraction pattern of the heat-treated fiber, which indicates the improvement of the crystallinity in the meridional direction [30]. Thus, it can be concluded that the single crystals of PPTAs are stabilized by the molecular chain movement in the chain direction after heat treatments.

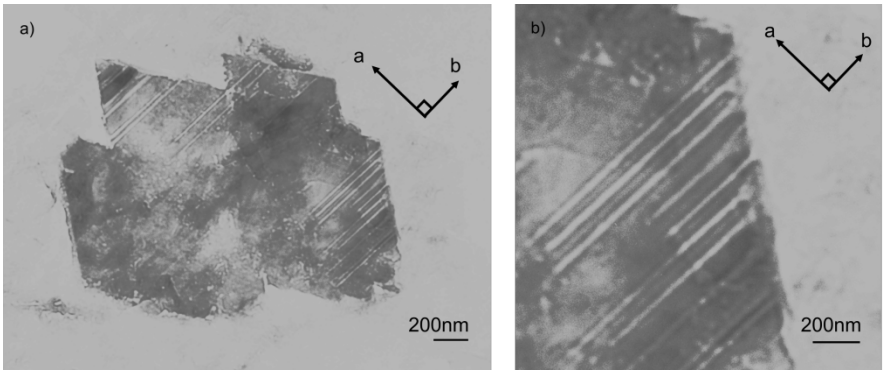


**Figure 5.** TEM image of a PPTA(32) single crystal after heat treatment at 350°C.

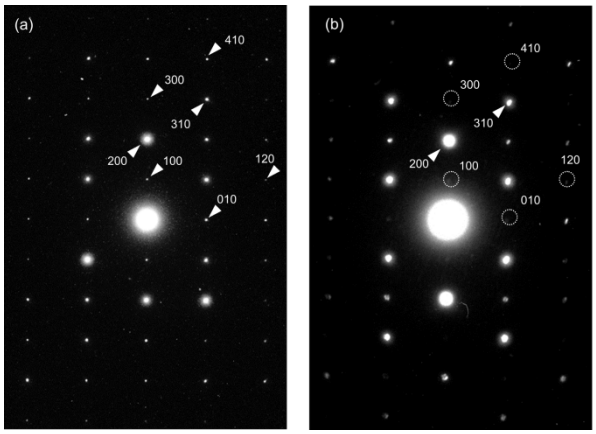


**Figure 6.** Electron diffraction patterns of a PPTA(32) single crystal.

a) as-crystallized and b) after heat treatment at 350°C.

Figure 7 shows high-resolution dark-field images of PPTA single crystals before and after the heat treatment. The sizes of the crystallites are quantified in Table 4. Narrow crystallites were observed in both samples, and the long axes of the narrow crystallites corresponded to the *b*-axis. In addition, the crystallites became larger after the heat treatment, particularly along the *b*-axis direction. In other words, during the heat treatment, the crystallites grew along the *b*-axis rather than the *a*-axis because the hydrogen bonds existed in the *b*-axis direction. These *b*-axis-grown crystallites were also reported in Dobb *et al.*'s fiber studies [14], as described in Introduction section. Based on this finding and the results of the electron diffraction, it was concluded that the PPTA single crystals were stabilized through the heat treatment and narrow crystallites grew in the hydrogen-bonding direction.

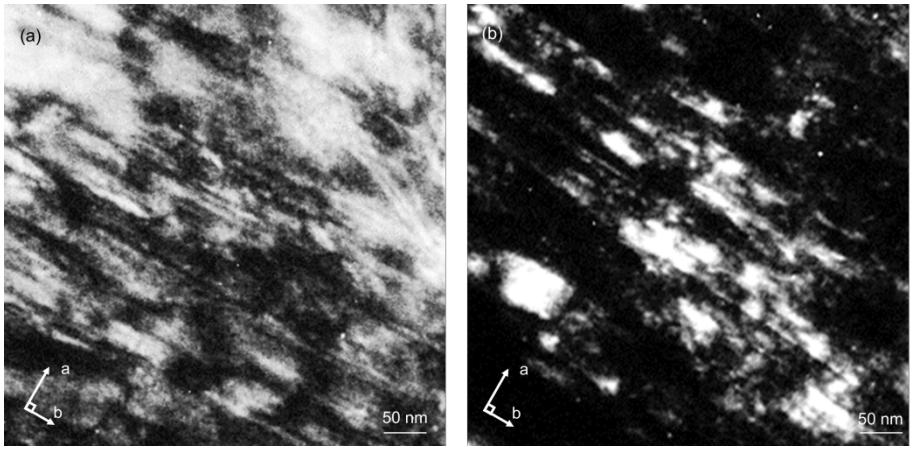


**Figure 7.** High-resolution dark-field images of PPTA(32) single crystals taken by the 200 reflection. a) as-crystallized and b) after heat treatment at 350°C.

**Table 4** Crystallite sizes of PPTA(32) single crystals measured from dark-field images taken by the 200 reflection.

| direction | Crystallite size | |
|---|---|---|
| | As-crystallized | Heat-treated |
| *a*-axis | 8.1 ± 1.9 nm | 11.1 ± 7.7 nm |
| *b*-axis | 51.6 ± 11.7 nm | 67.3 ± 20.0 nm |

The thickness of the heat-treated PPTA single crystals was consistent with that of the as-crystallized single crystals, and it was not changed by heat treatment as shown in Figure 8. This result differs from that obtained in the previously study [32], wherein the thickness of the single crystals of flexible polymers, such as polyethylene, increased upon heat treatment. Thus, it was proven that the thickness of the PPTA-extended chain crystals without folding did not increase even after heat treatment, and changes were observed in the crystal symmetry and the size of the crystallites increased in the hydrogen-bonding direction.

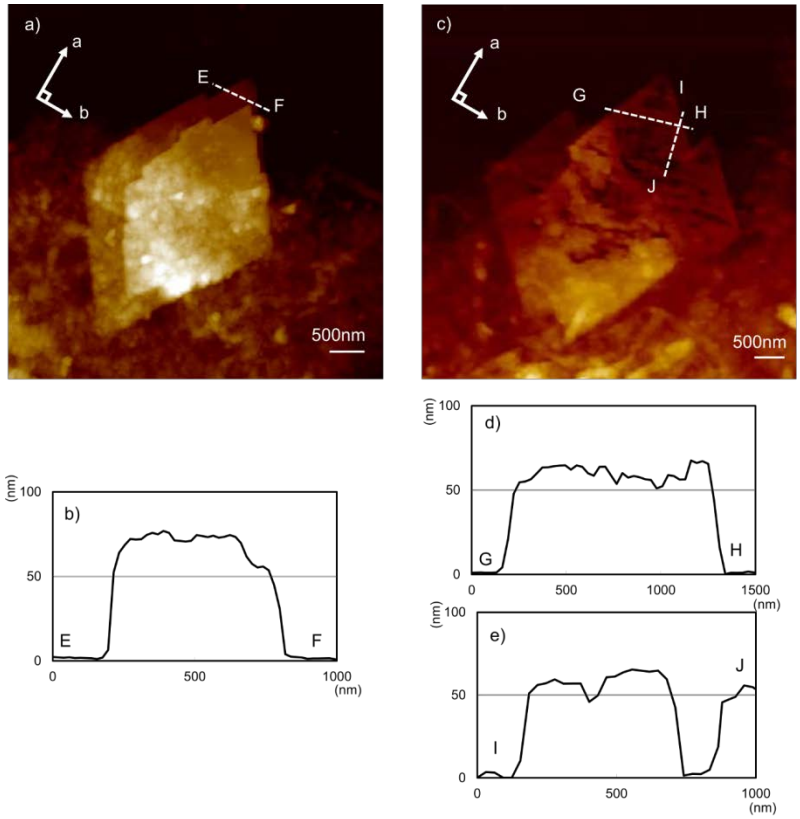


**Figure 8.** Scanning probe microscopy images and cross-sectional height profiles of PPTA single crystals. a) PPTA(60) single crystal prepared by the self-seeding method at 75°C, b) the cross-sectional height profile along the E–F line in a), c) PPTA(60) single crystal prepared by the self-seeding method at 75°C followed by heat treatment at 350°C and the cross-sectional height profiles along the lines d) G–H, and e) I–J in c).

## 3.3. Equilibrium Dissolution Temperature of PPTA Single Crystals

The $T_d$s of PPTA single crystals with different molecular lengths are detailed in Table 5. It was found that longer PPTA molecular chains have a higher $T_d$. The behavior is the same as that of the $T_d$ of the prepared PPTA crystal by isothermal crystallization at 0°C, as shown in

Table 2. However, the $T_d$ of the PPTA single crystal, which was prepared using a self-seeding method with a low degree of supercooling, is higher than that of the obtained PPTA crystal by utilizing conventional isothermal crystallization with a high degree of supercooling. This is because the PPTA single crystal is composed of a more stable modification I structure.

**Table 5.** $T_d$ of the prepared PPTA single crystals using the self-seeding method.

| Sample code | Dissolution temperature (°C) |
|---|---|
| PPTA(32) | 99.1 |
| PPTA(60) | 107.8 |
| PPTA(80) | 111.6 |

According to a study on flexible polymers by Lauritzen, Hoffman, Price [33, 34], the equilibrium $T_d$ (the $T_d$ of the crystal of infinite thickness, $T_d^0$) is obtained from the relationship between the $T_d$ and the thickness of the crystal. As described above, the thickness of each PPTA single crystal is identical to the average molecular chain length. Therefore, the $T_d^0$ of the PPTA single crystal can be estimated by comparing its $T_d$ and PPTA molecular chain length. Thus, the relation between the molecular chain length of the PPTA and the $T_d$ of PPTA single crystals can be established.

First, it is considered as a crystal model in which *n* molecular chains are extended, assuming that the crystal thickness is equal to the molecular chain length and that the cross-sectional area of a single molecular chain is *a* (Figure 9). In the crystallization from a dilute solution, the free energy change ($\Delta\varphi$) by the crystal formation is a summation of an increase in the surface free energy of the newly formed crystals and a decrease in the free energy due to the volume formation:

$$\Delta\varphi = A\sigma - V\Delta f,$$

where $\Delta f$ is the difference in the free energy between the solution and the crystal states of the molecular chain, $\sigma$ is the surface free energy per unit surface area, V is the volume, and A is the surface area.

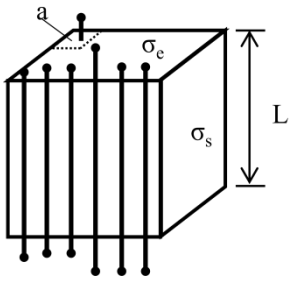


**Figure 9.** Schematic drawing of a PPTA crystal.

If $\sigma_e$ and $\sigma_s$ represent the surface free energy per unit surface area of the end and side faces, respectively, and C is the shape factor, $A\sigma$ and $\Delta f$ can be described as follows:

$$A\sigma = 2na\sigma_e + CnaL\sigma_s$$

$$\Delta f = \Delta h - T\Delta S,$$

where $\Delta h$ is the intermolecular aggregation energy based on the chemical structure of the molecular chain, and $\Delta S$ is the entropy change that is primarily attributed to the dissolution and the associated change in the molecular chain morphology. L is the length of the PPTA molecular chain.

Therefore,

$$\Delta\varphi = 2na\sigma_e + CnaL\sigma_s - naL\Delta f.$$

At $T_d$, $\Delta\varphi$ is equal to 0, therefore

$$T_d = A - B/L,$$

where $A = (\Delta h - C\sigma_s)/\Delta S$ and $B = 2\sigma_e/\Delta S$.

$T_d$ is linearly related to 1/L, and $T_d^0$ can be obtained by extrapolating the molecular chain length "L" to infinity. The $T_d$s of the PPTA single crystals are plotted versus the inverse of the molecular length, as shown in Figure 10, so a linear relation is obtained between the $T_d$ and 1/L. According to Figure 10, the $T_d^0$ of the PPTA single crystal in 78.5 wt% sulfuric acid was estimated to be 119.2°C.

From these results, the equilibrium dissolution temperature could be obtained by measuring the dissolution temperature of the PPTA single crystals. A linear relation was clearly obtained between the inverse of the thickness of the PPTA single crystal (i.e., the length of the PPTA chain used for the crystallization) and the dissolution temperature, and the dissolution temperatures of the PPTA single crystals in predetermined concentrations of sulfuric acid could be estimated through the length of the PPTA chain.

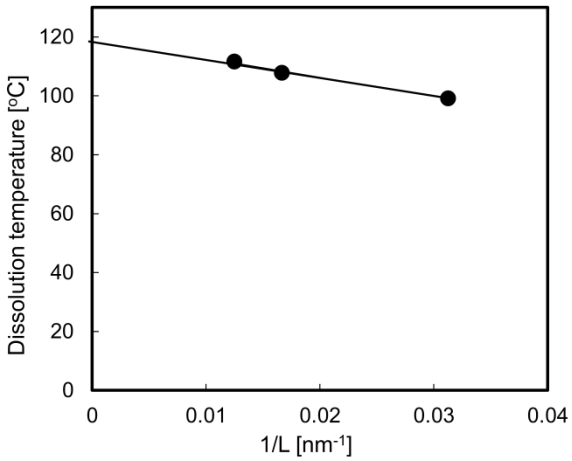


**Figure 10.** Dissolution temperatures of the PPTA single crystals in 78.5 wt% sulfuric acid as a function of the inverse of the polymer molecular length (1/L).

# 4. Conclusions

The isothermal crystallization of PPTA resulted in the formation of modification II PPTA crystals with plate-like morphologies and an unclear crystal habit. However, crystallization using a self-seeding method with a low degree of supercooling yielded lozenge-shaped modification I PPTA single crystals. In the obtained lozenge-shaped crystals, the *a*-axis direction corresponded to the long diagonal direction of the rhombus, the *b*-axis direction to the short diagonal direction, and the PPTA molecular chain axis (i.e., the *c*-axis direction) to the thickness direction of the crystal. The growth plane of the PPTA single crystal was the (110) plane, and the thickness of single crystals was approximately equal to the average molecular length of the PPTA used for the crystallization. It was considered that during the crystallization in the sulfuric acid solution, the effect of hydrogen bonding between the PPTA molecular chains was weakened by the interaction between the PPTA molecular chains and sulfuric acid, and the growth in the *b*-axis direction (the hydrogen-bonding direction) did not proceed predominantly. Thus, the (110) plane of the PPTA crystal is reflected on the growing surface. In addition, as the PPTA single crystal was composed of an extended molecular chain, the length of the PPTA chain used for crystallization was directly reflected in the thickness of the PPTA single crystals.

The heat treatment of the PPTA single crystals resulted in a symmetry change from the P1a1 symmetry to the more stable P11n symmetry. Therefore, the P11n symmetry crystal was denser than the P1a1 symmetry crystal. It was considered that the crystal densification following the heat treatment made it difficult for the crystal to maintain its original morphology and the van der Waals forces in the *a*-axis direction were weaker than the hydrogen bonding in the *b*-axis direction, resulting in the formation of cracks parallel to the *b*-axis direction. The narrow crystallites elongated in the *b*-axis direction were observed in

the heat-treated PPTA single crystals, indicating that the narrow crystallites grew in the hydrogen-bonding direction. In addition, unlike previously reported polyethylene single crystals, which comprised flexible molecules, the thickness of the PPTA single crystals, which comprised extended molecules, did not change following heat treatment. Thus, it was proven that the thickness of the PPTA-extended chain crystals without folding did not increase even after heat treatment, and changes were observed in the crystal symmetry and the size of the crystallites increased.

Furthermore, the equilibrium $T_d$ of the PPTA single crystals in 78.5 wt% sulfuric acid was estimated to be 119.2°C. The proposed method is also applicable to other rigid polymers that form extended-chain crystals; therefore, our study presents a method for determining the equilibrium $T_d$ of rigid polymers.

## Author contributions

The manuscript was written through contributions of all authors. All authors have given approval to the final version of the manuscript. All of the authors contributed equally.

## Declaration of competing interest

The authors declare that they have no known competing financial interests or personal relationships that could have appeared to influence the work reported in this paper.

## Appendix A. Supplementary data

Supplementary data to this article can be found online at ***

# References

(1) Kwolek, S. L.; Morgan, P. W.; Sorenson, W. R. Process of making wholly aromatic polyamides. U.S. Patent 3063966, Nov. 13, 1962.

(2) Gaymans, R. J.; Tijssen, J.; Karkema, S.; Bantjes, A. Elastic modulus in the crystalline region of poly(*p*-phenylene terephthalamide), Polymer 17 (1976) 517-518. https://doi.org/10.1016/0032-3861(76)90133-6.

(3) Wilfong, R. E.; Zimmerman, J. Strength and durability characteristics of Kevlar aramid fiber, J. Appl. Polymer Sci., Appl. Polym. Symp. 31 (1977) 1-21.

(4) Tashiro, K.; Kobyashi, M.; Tadokoro, H. Elastic moduli and molecular structures of several crystalline polymers, including aromatic polyamides, Macromol. 10 (1977) 413-420. https://doi.org/10.1021/ma60056a033.

(5) Northolt, M. G.; van Aartsen, J. J. Chain orientation distribution and elastic properties of poly (*p*-phenylene terephthalamide), a "rigid rod'' polymer, J. Polym. Sci. Polym. Symp. 58 (1977) 283-296. https://doi.org/10.1002/polc.5070580120.

(6) Northolt, M. G. Tensile deformation of poly(*p*-phenylene terephthalamide) fibres, an experimental and theoretical analysis, Polymer 21 (1980) 1199-1204. https://doi.org/10.1016/0032-3861(80)90088-9.

(7) Allen, S. R.; Roche E. J. Deformation behaviour of Kevlar® aramid fibres, Polymer 30 (1989) 996-1003. https://doi.org/10.1016/0032-3861(89)90069-4.

(8) Gan, L. H.; Blais, P.; Carlisson, D. J.; Suprunchuk, T.; Wiles, D. M. Physicochemical characterization of some fully aromatic polyamides, J. Appl. Polym. Sci. 19 (1975) 69-82. https://doi.org/10.1002/app.1975.070190106.

(9) Kapuscinska, M.; Pearce, E. M. Aromatic polyamides. XI. Effect of the halogen substitution on the thermal and flammability behavior of poly(1,4-phenylene terephthalamide), J. Polym. Sci. Polym. Chem. Ed. 22 (1984) 3989-3998. https://doi.org/10.1002/polb.1995.090330101.

(10) Lee, K. G.; Barton, R. Jr.; Schultz, J. M.; Structure and property development in poly(*p*-phenylene terephthalamide) during heat treatment under tension, J. Polym. Sci., B, Polym. Phys. 33 (1995) 1-14. https://doi.org/10.1002/pol.1973.130110508.

(11) Northolt, M. G.; van Aartsen J. J. On the crystal and molecular structure of poly-(*p*-phenylene terephthalamide), J. Polym. Sci., B, Polym. Phys. 11 (1973) 333-337. https://doi.org/10.1016/0014-3057(74)90131-1.

(12) Northolt M. G. X-ray diffraction study of poly(*p*-phenylene terephthalamide) fibers, Eur. Polym. J. 10 (1974) 799-804. https://doi.org/10.1002/app.1979.070230326.

(13) Haraguchi, K.; Kajiyama, T.; Takayanagi, M. Effect of coagulation conditions on crystal modification of poly(p-phenylene Terephthalamide), J. Appl. Polym. Sci. 23 (1979) 915-926. https://doi.org/10.1002/app.1979.070230326.

(14) Dobb, M. G.; Johnson, D. J.; Saville, B. P. Supramolecular structure of a high-modulus polyaromatic fiber (Kevlar 49), J. Polym. Sci. Polym. Phys. Ed. 15 (1977) 2201-2011. https://doi.org/10.1002/pol.1977.180151212.

(15) Liu, J.; Cheng, S. Z. D.; Geil, P. H. Morphology and crystal structure in single crystals of poly(*p*-phenylene terephthalamide) prepared by melt polymerization, Polymer 37 (1996) 1413. https://doi.org/10.1016/0032-3861(96)81140-2.

(16) Takahashi, T.; Iwamoto, H.; Inoue, K. Quiescent and strain-induced crystallization of poly(*p*-Phenylene Terephthalamide) from sulfuric acid solution, J. Polym. Sci. Polym. Phys. Ed. 17 (1979) 115-122. https://doi.org/10.1002/pol.1979.180170111.

(17) Jackson, C. L.; Chanzy, H. D. Morphology and structure of poly(*p*-phenylene terephthalamide) crystallized from dilute organic solution, Polymer 34 (1993) 5011-5015. https://doi.org/10.1016/0032-3861(93)90242-3.

(18) Horio, M.; Kaneda, T.; Ishikawa, S.; Shimamura, K. Morphology of fibers made from polymer liquid crystals, Sen'i Gakkaishi 40 (1984) 285-290. https://doi.org/10.2115/fiber.40.8_T285.

(19) Baird, D. G.; Smith, J. K. Dilute solution properties of poly(1,4-phenylene terephthalamide) in sulfuric acid, J. Polym. Sci. 16 (1978) 61-70. https://doi.org/10.1002/pol.1978.170160106.

(20) Takahashi, T.; Yamamoto, T.; Tsujimoto, I. Morphology of poly(*p*-phenylene terephthalamide) precipitated from hexamethylphosphoric triamide/N-methylpyrrolidone-2/lithium chloride solutions, J. Macromol. Sci. Part B-Phys. B16 (1979)539-549.

(21) Blundell, D. J.; Keller, A.; Kovacs, A. J. A new self-nucleation phenomenon and its application to the growing of polymer crystals from solution, J. Polym. Sci. B4 (1966) 481-486. https://doi.org/10.1002/pol.1966.110040709.

(22) Shimamura, K.; Uchida, T.; Suzuki, M.; Zhang, C. Crystallization of poly (*p*-phenylene benzobis-oxazole) from dilute solution, Sen'i Gakkaishi 54 (1998) 374-378. https://doi.org/10.2115/fiber.54.7_374.

(23) Shimamura, K.; Uchida, T. Morphology and structure of poly(*p*-phenylene Benzobisthiazole) crystals, J. Macromol. Sci. Part B-Phys. B39 (2000) 667-677.

(24) Shimamura, K.; Uchida, T. Observation of a solitary rigid molecular chain cilium standing on poly(*p*-phenylene benzobisthiazole) lamellar crystal, J. Macromol. Sci. Part B-Phys. B41 (2002) 529-537.

(25) Shimamura, K.; Michiaki, N.; Ikeda, T.; Uchida, T.; Hirao, M. Fractionation and crystal morphology of rigid polymer, poly(*p*-phenylene benzobisthiazole) , J. Macromol. Sci. Part B-Phys. B43 (2004) 1015-1024.

(26) Xu, D.; Okuyama, K.; Kumamaru, F.; Takayanagi, M. Morphorogical and Structural Studies on Large Spherulites of Poly(*p*-phenylene terephthalamide), Polym. J. 16 (1984) 31-40. https://doi.org/10.1295/polymj.16.31.

(27) Keller, A. A note on single crystals in polymers: evidence of a folded-chain configuration, Phil. Mag. 2 (1957) 1171-1175. https://doi.org/10.1080/14786435708242746.

(28) Niegisch, W. D.; Swan, P. R. Hollow pyramidal crystals of polyethylene and a mechanism of growth, J. Appl. Phys. 31 (1960) 1906-1910. https://doi.org/10.1063/1.1735472.

(29) Haraguchi, K.; Kajiyama, T.; Takayanagi M. Dynamic mechanical property of poly(*p*-phenylene terephthalamide) fiber, Sen'i Gakkaishi 33 11 (1977) 535-540. https://doi.org/10.2115/fiber.33.11_T535.

(30) Kunugi, T.; Watanabe H.; Hashimoto M. Dynamic mechanical property of poly(*p*-phenylene terephthalamide) fiber, J. Appl. Polymer. Sci. 24 (1979) 1039-1051

https://doi.org/10.1002/app.1979.070240417

(31) Hindeleh A.M. ; Abdo Sh. M. Effects of annealing on the crystallinity and microparacrystallite size of Kevlar 49 fibers, Polymer 30 (1989) 218-224

https://doi.org/10.1016/0032-3861(89)90108-0

(32) Hirai, N.; Mitsuhata, T.; Yamashita, Y. Thickening process of polyethylene single crystals by heat treatment I, Koubunshi Kagaku 18 (1961) 33-38. https://doi.org/10.1295/koron1944.18.33

(33) Lauritzen, J.; Hoffman, J. D. Theory of formation of polymer crystals with folded chains in dilute solution, J. Res. NBS. 64A (1960) 73-102.

(34) Price, F. P. The growth habit of single polymer crystals, J. Polym. Sci. 42 (1960) 49-56. https://doi.org/10.1002/pol.1960.1204213906.

# Supporting Information for:

Preparation of solution-grown lozenge-shaped poly(*p*-phenylene terephthalamide) single crystals and their structural stabilization by heat treatment

Tetsuya Uchida*, Yutaro Hara, Tomoyasu Takaki
* Corresponding author. Graduate School of Natural Science and Technology,
Okayama University, 3-1-1 Tsushima-naka, Kita-ku Okayama 700-8530, Japan
E-mail address: tuchida@cc.okayama-u.ac.jp (T.Uchida)

**Hydrolysis of the PPTA fiber**

The samples were prepared for infrared (IR) spectrometry measurements by the KBr method. The IR measurements were conducted using a PARAGON 1000 FT IR instrument (Perkin Elmer, Inc., MA, USA).

Fig. S1 shows the infrared (IR) spectra of the PPTA fibers before and after hydrolysis. Because the characteristic peaks corresponding to the amide groups of PPTA (1525 and 1660 $cm^{-1}$) were observed both before and after hydrolysis, it was concluded that the basic structure of the PPTA was not affected by the hydrolysis process.

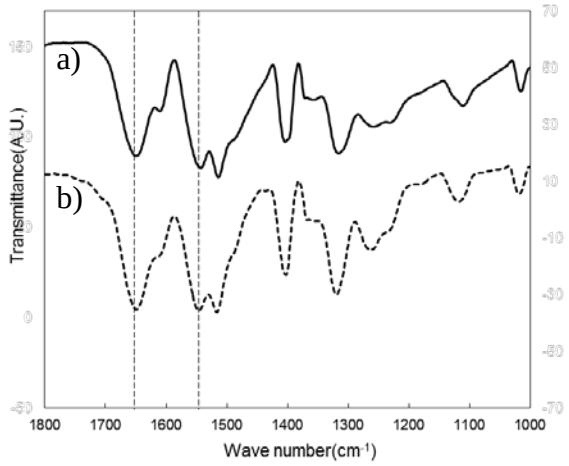


**Fig. S1** Infrared spectra of (a) a PPTA fiber and (b) PPTA hydrolyzed for 78 h.

**Table S1. Observed and calculated lattice spacings for the samples shown in Fig. 1d**

(vs = very strong, s = strong, m = medium, w = weak, and vw = very weak)

| *h k l* | $d_{obs.}$(nm) | $d_{calc.}$(nm) | Intensity |
|---|---|---|---|
| 0 1 0 | $0.51_6$ | 0.522 | s |
| 2 0 0 | $0.39_1$ | 0.394 | s |
| 2 1 0 | $0.30_9$ | 0.314 | m |

**Table S2. Observed and calculated lattice spacings for the samples shown in Fig. 2b**

(vs = very strong, s = strong, m = medium, w = weak, and vw = very weak)

| *h k l* | $d_{obs.}$(nm) | $d_{calc.}$ (nm) | Intensity |
|---|---|---|---|
| 0 1 0 | $0.51_8$ | 0.522 | vw |
| 1 1 0 | $0.43_9$ | 0.435 | s |
| 2 0 0 | $0.39_6$ | 0.394 | vs |
| 2 1 0 | $0.31_8$ | 0.314 | m |

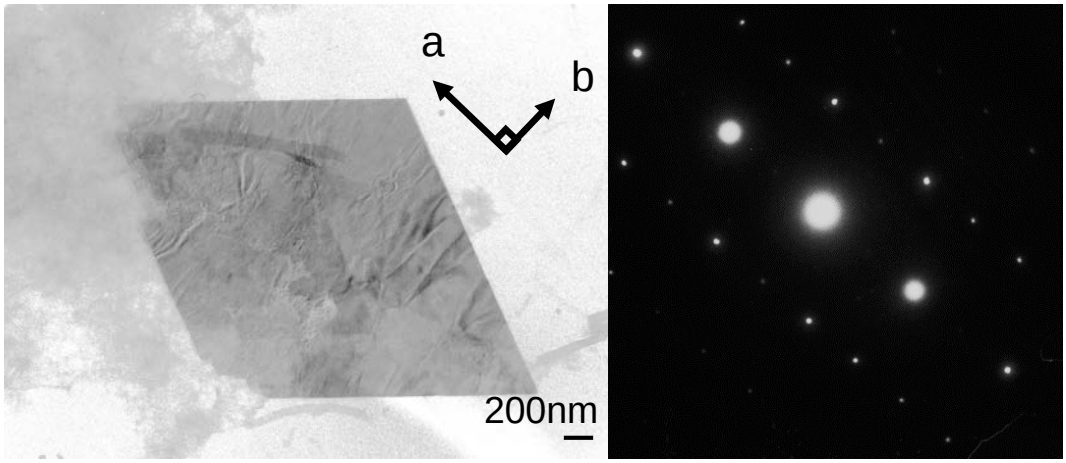


**Fig. S2** Transmission electron microscopy and electron diffraction of PPTA single crystals. a) PPTA(60) single crystal prepared by self-seeding method at 65°C and b) electron diffraction from selected area in a).

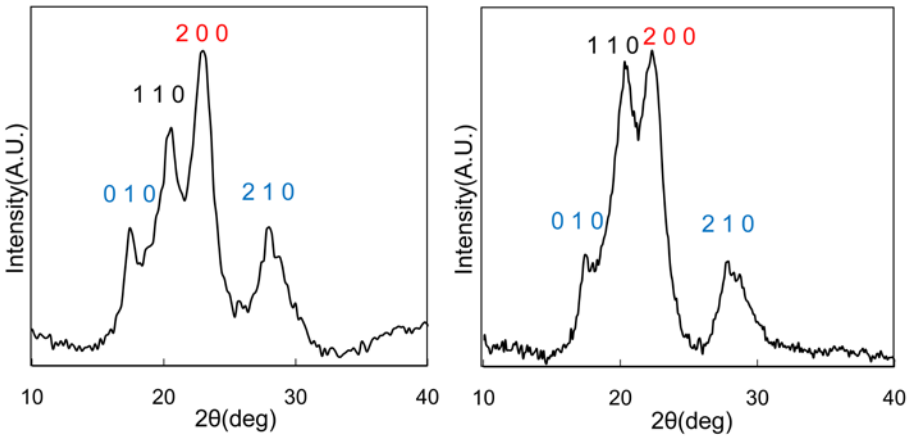


**Fig.S3** X-ray diffraction patterns of PPTA single crystals.

a) as crystallized and b) after heat treatment at 400°C.

These measurements were conducted using a VariMax Rapid instrument (Rigaku Co., Tokyo, Japan).